

Xi Wang

Jian Cao

e-mail: jcao@northwestern.edu

Department of Mechanical Engineering,  
Northwestern University,  
Evanston, IL 60208

# Wrinkling Limit in Tube Bending

*Thin-walled tube bending has found many of its applications in the automobile and aerospace industries. This paper presents an energy approach to provide the minimum bending radius, which does not yield wrinkling in the bending process, as a function of tube and tooling geometry and material properties. A doubly-curved sheet model is established following the deformation theory. This approach provides a predictive tool in designing/optimizing the tooling parameters in tube bending. [DOI: 10.1115/1.1395018]*

## Introduction

A tube possesses a combination of light weight and high stiffness, which has attracted many applications in the aerospace, automobile, oil and various other industries. In the auto industry, for example, tube hydroforming has been identified as one of the key technologies to reduce vehicle weight while increasing the stiffness and integrity of automobiles [1]. A crucial challenge in hydroforming is the optimization of tool and process conditions. A typical tube hydroforming process, like manufacturing exhaust manifolds, engine cradles and frames, involves bending of tubes as the first step followed by hydroforming in a closed die. During the rotary-draw tube bending shown in Fig. 1 (Stelson and Lou [2]), the clamp die holds the tube which is bent tightly against the bending die at the leading end of the bender. The pressure die deforms the tube into the desired shape. A mandrel is used to support the inside of the tube and prevent the collapse of the tube (Li et al. [3]). As a result of bending, axial compressive stress is developed in the tube section near the bending die. Thus, local wrinkles may be initiated, as wrinkling is a phenomenon of compressive instability. The deformation and springback in rotary-draw tube bending has been studied by Li and Stelson [3], Stelson and Lou [2], etc. However, the wrinkling problem in tube bending has not received much attention. Current industrial practice is to add enough design tolerance into the problem so that no wrinkles will be formed in tube bending. With the ever-increasing demand of low-cost manufacturing and design for manufacturability, a reliable prediction tool is needed.

Research efforts on the prediction of wrinkling have been made in the last fifty years. The analytical solution can provide a global view in terms of the general tendency and the effect of individual parameters on the onset of wrinkling and can be achieved in an almost negligible computational time. However, past analytical work has concentrated on some relatively simple problems such as a column under axial loading (Shanley [4]), a circular ring under inward tension, and an annular plate under bending with a conical punch at the center, etc. Plastic bifurcation analysis is one of the most widely used analytical approaches to predict the onset of wrinkling. Hutchinson and Neale [5] and Neale and Tuğcu [6] studied bifurcation phenomenon of doubly curved sheet metal by adopting Donnell-Mushtari-Vlasov (DMV) shell approximations. The investigation was applicable to the regions of the sheet which are free of any surface contact. However, all the above analyses neglected the boundary condition along the edge of the region being examined for wrinkling. Fatnassi et al. [7] performed a theoretical investigation to predict the nonaxisymmetric buckling in the throat of circular elastic-plastic tubes subjected to a nosing operation along a frictionless conical die. The buckling point and associated modes are determined by Hill's bifurcation theory in conjunction with a nonaxisymmetric buckling mode.

Pure bending of inelastic cylindrical shells have been carried out experimentally and numerically by Corona and Kyriakides

[8], Kyriakides and Ju [9], etc. A thinner shell was found to develop short wavelength periodic ripples on the compressed side of the shell (as shown in Fig. 2) and the shell buckled locally and collapsed soon after the appearance of the wrinkles. Therefore, thin-walled shell bending is limited by various shell buckling modes in addition to the limit load instability. Ju and Kyriakides [10] numerically investigated the instabilities of long circular shell bending, which involves bifurcation into short wavelength ripples, localization following a natural limit load and interaction of the two. They used Sanders' shell kinematics and the principle of virtual work to simulate the growth of axial ripples and the localization phenomena. Corona and Vaze [11] addressed the response, which was buckling and collapse of long thin-walled square tubes under pure bending, analytically and experimentally. Rayleigh-Ritz type formulations were developed based on the principle of virtual work to predict the response of the tubes and the critical curvature at which the ripples appear. As shown in Fig. 1, the bent tube is restricted by tooling and it is found that the boundary restrictions over the examined area for wrinkling are very critical to the onset of wrinkles in the previous work (Wang and Cao [12–14]). However, these above studies are concerned with long shells without any boundary restriction at the ends.

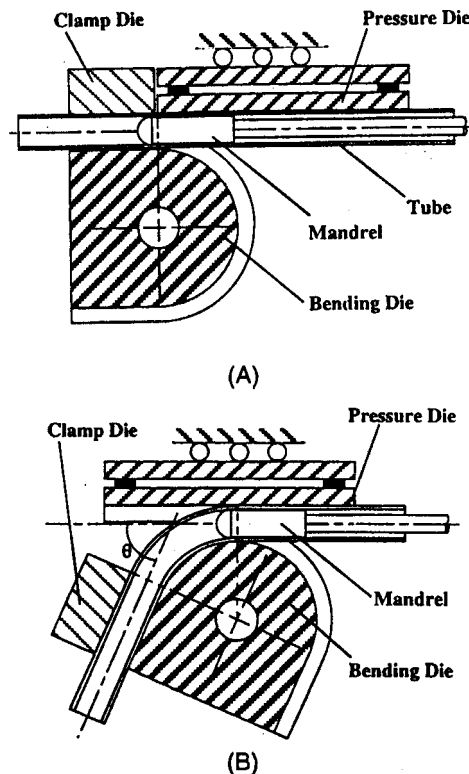
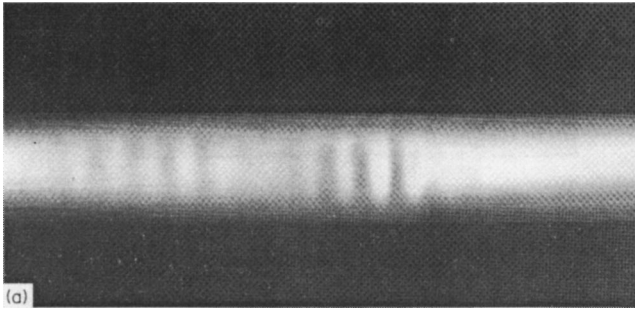


Fig. 1 Rotary-draw bending with mandrel (Stelson [2])

Contributed by the Materials Division for publication in the JOURNAL OF ENGINEERING MATERIALS AND TECHNOLOGY. Manuscript received by the Materials Division July 25, 2000. Guest Editors: Jian Cao and Z. Cedric Xia.



**Fig. 2 Wrinkling on compression side of shell in pure bending (Ju and Kyriakides [9])**

The energy method has been another approach to analytically investigate the buckling problem such as flange wrinkling in Cao and Wang [15], Wang and Cao [16], etc. Recently, Wang and Cao [12–14] proposed a wrinkling criterion for sheet wrinkling without normal constraints by using an energy approach considering the boundary restrictions of the examined area. They applied this approach to the cases of a straight side-wall and a curved wall with an infinite curvature in another direction in sheet metal forming processes. The predictions agreed very well with experimental results in all the cases examined. In this paper, we aim to extend this approach to the sheet with double curvatures, i.e., the wrinkling problem in tube bending.

In the present paper, an energy approach is established to provide a stress-based criterion for the general double-curvature sheet under compression. The effective dimensions over the region undergoing compressive hoop stress are introduced as dimension parameters. The critical buckling stress is obtained as a function of local curvatures, material properties, geometrical dimensions, and stress ratio. This criterion is then used to predict the onset of wrinkling in tube bending. The effects of tube thickness, tube radius and material properties on the minimum bending radius without the occurrence of wrinkling are discussed.

### General Wrinkling Criterion

This section aims to establish a general wrinkling criterion for the onset of wrinkling in the doubly curved sheet under a plane stress condition. In the following analysis, the prebuckling stress state in the sheet over the region examined for wrinkling is assumed to be at membrane state, and thus, the shear strains and stresses are ignored. All the formulations are developed within the context of thin plate and shell theory, therefore, the thickness of the sheet and all the stress states through the thickness are assumed to be uniform before buckling. Strains are expected to be small and the characteristic wavelength is large compared to sheet thickness and yet small compared to the radii of the curvatures of the sheet such that the strain measures given by Donnell-Mushtari-Vlasov (DMV) approximations can be adopted. Deformation theory is employed in the analysis since proportional loading before buckling is assumed.

The energy method has been extensively employed in Timoshenko [17] to study the elastic buckling of thin plates and shells with various boundary conditions. In his energy approach, a deflected form may be assumed for the plate and the critical buckling condition can be assessed by equating the internal energy of the buckled plate,  $\Delta U$ , and the work done by the in-plane membrane forces,  $\Delta T$ . If the internal energy for every possible assumed deflection is larger than the work produced by membrane forces, the sheet is considered under a stable equilibrium condition. Hence, the stability condition can be expressed as

$$\Delta T \leq \Delta U \quad (1)$$

To obtain the internal energy for every possible assumed deflection, the formulations for a general doubly curved sheet are

employed as detailed in Hutchinson and Neale [5] and Neale and Tugcu [6]. At the instant of buckling, the in-plane components of Lagrangian strain tensor  $\varepsilon_{\alpha\beta}$  at a distance  $x_3$  from the middle surface of the curved sheet can be approximated by

$$\varepsilon_{\alpha\beta} = E_{\alpha\beta} + x_3 \kappa_{\alpha\beta} \quad (2)$$

where the Greek indices range from 1 to 2,  $E_{\alpha\beta}$  and  $\kappa_{\alpha\beta}$  represent the stretching and bending strain which are given by

$$E_{\alpha\beta} = \frac{1}{2}(u_{\alpha,\beta} + u_{\beta,\alpha}) + b_{\alpha\beta} w \quad (3)$$

$$\kappa_{\alpha\beta} = -w_{,\alpha\beta}$$

where a comma denotes covariant differentiation with respect to in-plane coordinates  $(x_1, x_2)$ ,  $u_\alpha$  and  $w$  are the displacements in the in-plane direction  $(x_1, x_2)$  and the buckling deflection normal to the middle surface of the sheet,  $b_{\alpha\beta}$  is the curvature tensor of the middle surface in the prebuckling state. If a 3-D constitutive law with the form of  $\sigma_{\alpha\beta} = \bar{L}_{\alpha\beta\kappa\gamma} \varepsilon_{\kappa\gamma}$  is adopted, where the moduli  $\bar{L}_{\alpha\beta\kappa\gamma}$  are defined in the Appendix, the relationships for the membrane stress resultants can be given by

$$N_{\alpha\beta} = \int_{-t/2}^{t/2} \sigma_{\alpha\beta} dx_3 = t \bar{L}_{\alpha\beta\kappa\gamma} E_{\kappa\gamma} \quad (4)$$

and the bending moments are given by

$$M_{\alpha\beta} = \int_{-t/2}^{t/2} \sigma_{\alpha\beta} x_3 dx_3 = \frac{t^3}{12} \bar{L}_{\alpha\beta\kappa\gamma} \kappa_{\kappa\gamma} \quad (5)$$

The internal energy under the assumption of DMV thin plate and shell theory can be obtained as

$$\Delta U = \int_S \left( \int M_{\alpha\beta} d\kappa_{\alpha\beta} + N_{\alpha\beta} dE_{\alpha\beta} \right) dS \quad (6)$$

where  $S$  is the region of the sheet's middle surface over which the wrinkles occur. By assuming the virtual displacements  $u_\alpha = 0$  and using the deformation theory, Eq. (6) can be simplified as

$$\Delta U = \frac{t^3}{24} \int_S \bar{L}_{\alpha\beta\kappa\gamma} w_{,\kappa\gamma} w_{,\alpha\beta} dS + \frac{t}{2} \int_S \bar{L}_{\alpha\beta\kappa\gamma} b_{\alpha\beta} b_{\kappa\gamma} w^2 dS \quad (7)$$

The external work done by the membrane forces acting in the middle plane of the sheet is represented as

$$\Delta T = \frac{1}{2} \int_S (N_{11} w_{,1}^2 + N_{22} w_{,2}^2) dS \quad (8)$$

For a thin curved sheet, the boundary condition or continuity condition along the edges of the region being examined for wrinkling strongly affects the critical buckling condition since the admissible deflection mode will be different. By appropriately choosing the deflection form to reflect the boundary restriction and equating the energy  $\Delta U = \Delta T$ , the critical conditions can be calculated analytically as a function of in-plane stress, material properties, and geometry parameters.

Generally, the energy equality is considered over the entire region being examined and the stress field before wrinkling is assumed to be uniform over the entire region. However, from our previous work on flange wrinkling and side-wall wrinkling in sheet metal forming, it is demonstrated that the dimensions of the effective compressive area are critical to the initiation of wrinkles. Therefore, this effective area will be implemented in the above energy integration in Eqs. (7)–(8).

### Buckling Condition in Tube Bending

A typical tube used in tube bending, as shown in Fig. 1, has a ratio of tube diameter ( $2r$ ) to tube thickness ( $t$ ) greater than 10 and is bent around the bending die with the radius of  $R_d$ . Hence,

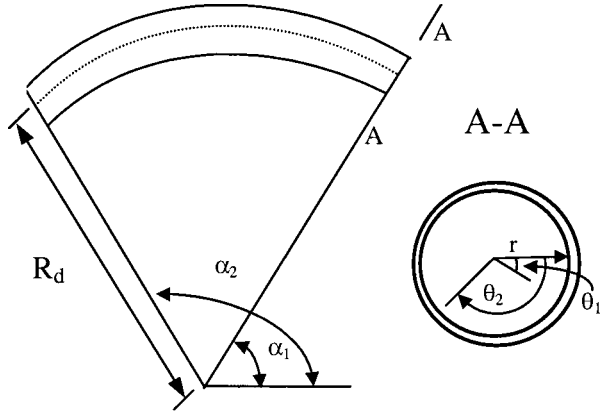


Fig. 3 Schematic of curved sheet model in tube bending

the thin-shell assumption employed in the previous section is suitable. The thin-walled sheet in the bending area is free of internal pressure leading to the assumption of under plane stress deformation. The mandrel acts to provide a near-perfect clamping condition at the end and therefore, considering its effective compressive area, the tube is simplified as a clamped curved sheet within  $(\alpha_1, \alpha_2)$  and  $(\theta_1, \theta_2)$  in two curvilinear directions as shown in Fig. 3.

The normal deflection,  $w$ , satisfies the following boundary conditions

$$\begin{aligned} w=0, \frac{\partial w}{\partial \alpha}=0, \quad \text{at } \alpha=\alpha_1, \alpha_2 \\ w=0, \frac{\partial w}{\partial \theta}=0, \quad \text{at } \theta=\theta_1, \theta_2 \end{aligned} \quad (9)$$

Thus, the deflection of the plate is assumed to be of the form

$$w=w_0 \left( 1 - \cos \left( 2m\pi \frac{\theta - \theta_1}{\theta_2 - \theta_1} \right) \right) \left( 1 - \cos \left( 2n\pi \frac{\alpha - \alpha_1}{\alpha_2 - \alpha_1} \right) \right) \quad (10)$$

where  $m$  is the wave number along the circumferential direction of the tube and  $n$  is the wave number in the  $\alpha$  direction. Having Eq. (10) as the assumed deflection form, the internal energy  $\Delta U$  becomes

$$\begin{aligned} \Delta U = \frac{t^3}{24} \int_{\alpha_1}^{\alpha_2} \int_{\theta_1}^{\theta_2} \left\{ \bar{L}_{2222} \left( \frac{\partial^2 w}{r^2 \partial \theta^2} \right)^2 + \bar{L}_{3333} \left( \frac{1}{R'^2} \frac{\partial^2 w}{\partial \alpha^2} - \frac{\cos \theta}{r^2} \frac{\partial w}{\partial \theta} \right)^2 \right. \\ + 2\bar{L}_{2233} \frac{\partial^2 w}{r^2 \partial \theta^2} \left( \frac{1}{R'^2} \frac{\partial^2 w}{\partial \alpha^2} - \frac{\cos \theta}{r^2} \frac{\partial w}{\partial \theta} \right) + 4\bar{L}_{2323} \left( \frac{1}{rR'} \frac{\partial^2 w}{\partial \theta \partial \alpha} \right. \\ + \frac{\cos \theta}{R'^2} \frac{\partial w}{\partial \alpha} \left. \right)^2 + \frac{12}{t^2} \left( \bar{L}_{2222} \left( \frac{w}{r} \right)^2 + \bar{L}_{3333} \left( \frac{w}{R'} \right)^2 \right. \\ \left. + \bar{L}_{2233} \frac{w^2}{R'r} \right) \left. \right\} R' r d\theta d\alpha \quad (11) \end{aligned}$$

where  $R' = (R_d - r \sin \theta)$

With the stress resultants  $N_{11} = -t\sigma_r$  and  $N_{22} = -t\sigma_\theta$ , the external work done by the membrane forces acting in the middle plane yields

$$\Delta T = -\frac{t}{2} \int_{\alpha_1}^{\alpha_2} \int_{\theta_1}^{\theta_2} \left\{ \sigma_\theta \left( \frac{1}{r} \frac{\partial w}{\partial \theta} \right)^2 + \sigma_\alpha \left( \frac{1}{R'} \frac{\partial w}{\partial \alpha} \right)^2 \right\} R' r d\theta d\alpha \quad (12)$$

By substituting the assumed deflection in Eq. (10) into Eqs. (11) and (12), the energy equality  $\Delta T = \Delta U$  yields the solution for the critical condition on the onset of wrinkling. In the case that

$\Delta T$  is always less than  $\Delta U$  for all the admissible deflection forms, no wrinkling would develop at that bending condition, i.e., bending radius  $R_d$ .

## Numerical Analysis and Results

**Critical Die Radius.** The analytical model for the bent tube section between the clamping die and pressure die or mandrel (as shown in Fig. 1) can be treated as a pure bending problem. For simplicity, the thickness variation is ignored, i.e., the out-of-plane strain  $\varepsilon_z = 0$ . Therefore, for the large deformation of the bent tube, we have strain  $\varepsilon_\alpha$  in the bending direction and circumferential strain  $\varepsilon_\theta$  as

$$\varepsilon_\theta = -\varepsilon_\alpha = \ln(R'/R_d) \quad (13)$$

The material is characterized as an elastic-plastic material following Swift's law  $\bar{\sigma} = K(\bar{\varepsilon} + \varepsilon_0)^n$ . Hill's 1948 yield criterion is employed to describe the normal anisotropic behavior of the material and the anisotropy parameter  $R$  is defined as the ratio of plastic strain in the width direction to plastic strain through thickness in a uniaxial tensile test. Thus, the stress distribution can be derived as

$$\sigma_\theta = -\sigma_\alpha = \sqrt{\frac{1+R}{2}} K \left( \sqrt{\frac{2(1+R)}{1+2R}} |\ln(R'/R_d)| + \varepsilon_0 \right)^n \quad (14)$$

From Eq. (13), it can be seen that the range of  $\theta$  in the effective compressive area is between  $(0, \pi)$ . By choosing  $\alpha_1 = 0$ , we have  $\alpha_2 = \Delta\alpha$ , which is the bending angle. In addition, it is found numerically that the minimum stress exists when the wave number in the circumferential direction  $m$  equals to 1. By substituting these simplifications into Eqs. (11)–(12), we obtain the energy functional

$$F = \Delta U - \Delta T = I_{n4} n^4 + \left( I_{n2} + \frac{12}{t^2} I_\alpha \right) n^2 + \left( I_{n0} + \frac{12}{t^2} I_\theta \right) = 0 \quad (15)$$

where

$$I_\theta = \int_0^\pi \frac{6R'\Delta\alpha}{r} \sin^2 2\theta \sigma_\theta d\theta \quad (16a)$$

$$I_\alpha = \int_0^\pi \frac{2\pi^2 r}{\Delta\alpha R'} (1 - \cos 2\theta)^2 \sigma_\alpha d\theta \quad (16b)$$

$$I_{n4} = \int_0^\pi \left( \frac{8\pi^4 r}{R'^3 \Delta\alpha^3} (1 - \cos 2\theta)^2 \right) \bar{L}_{3333} d\theta \quad (16c)$$

$$\begin{aligned} I_{n2} = \int_0^\pi \left( \left( -\frac{8\pi^2 \cos \theta}{R' r \Delta\alpha} (1 - \cos 2\theta) \sin 2\theta \cos \theta \right) \bar{L}_{3333} \right. \\ + \left( \frac{16\pi^2}{r R' \Delta\alpha} \cos 2\theta (1 - \cos 2\theta) \right) \bar{L}_{2233} + \frac{8\pi^2 r}{R' \Delta\alpha} \left( \frac{2}{r} \sin 2\theta \right. \\ \left. + \frac{\cos \theta}{R'} (1 - \cos 2\theta) \right) \bar{L}_{2323} \left. \right) d\theta \quad (16d) \end{aligned}$$

$$\begin{aligned} I_{n0} = \int_0^\pi \left( \left( \frac{24R'\Delta\alpha}{r^3} \cos^2 2\theta + \frac{18R'\Delta\alpha}{t^2 r} (1 - \cos 2\theta)^2 \right) \bar{L}_{2222} \right. \\ + \left( \frac{6R'\Delta\alpha \sin^2 2\theta \cos^2 \theta}{r^3} + \frac{18r\Delta\alpha (1 - \cos 2\theta)^2}{t^2 R'} \right) \bar{L}_{3333} \\ \left. + \left( \frac{12R'\Delta\alpha \cos \theta \sin 4\theta}{r^3} + \frac{18\Delta\alpha}{t^2} (1 - \cos 2\theta)^2 \right) \bar{L}_{2233} \right) d\theta \quad (16e) \end{aligned}$$

The energy function in Eq. (15) is a function of die radius  $R_d$ , wave number  $n$  as well as material properties, thickness and ge-

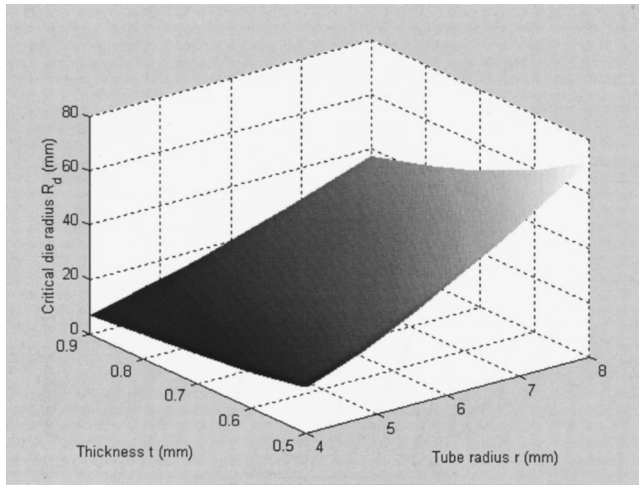


Fig. 4 Profile of critical die radius for AA6061-T6

ometry parameters such as local curvatures. The critical condition on the onset of wrinkling means that the energy equality function in Eq. (15) has a nontrivial solution for wave number  $n$ , which yields

$$\Delta = \left( I_{n2} + \frac{12}{t^2} I_{\alpha} \right)^2 - 4 * I_{n4} * \left( I_{n0} + \frac{12}{t^2} I_{\theta} \right) \geq 0 \quad (17)$$

The Eq. (17) under  $\Delta=0$  gives the minimum bending radius  $R_{d_{cr}}$  at which the wrinkles would not be initiated during the tube bending, which is defined as the critical die radius. The corresponding wave number is calculated as the critical wave number

$$n_{cr} = \sqrt{\left( I_{n2} + \frac{12}{t^2} I_{\alpha} \right) / 2 I_{n4}} \quad (18)$$

**Effects of Geometry and Material Properties.** From the above analysis it appears that the critical conditions at which wrinkling occurs in the bent tube, i.e., the critical die radius and critical wavelength, are affected by the tube radius, tube thickness and material properties. The understanding of these relationships will be helpful to prevent wrinkling during tube bending processes.

Figures 4 and 5 show the profiles of critical die radius versus tube radius and sheet thickness for different materials. The material used in Fig. 4 is AA6061-T6 with  $K=410$  MPa,  $n=0.085$ ,

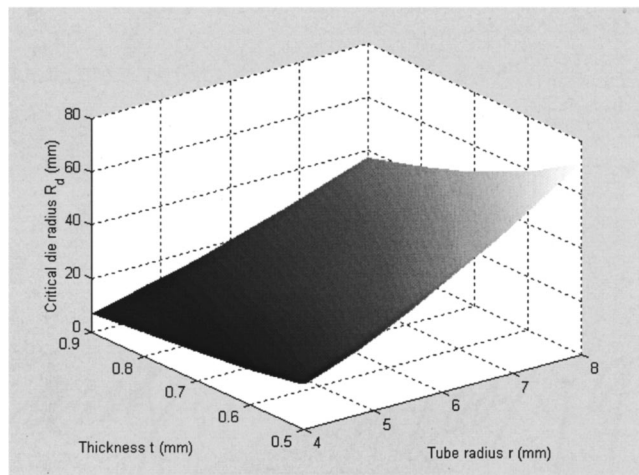


Fig. 5 Profile of critical die radius for 304 stainless steel

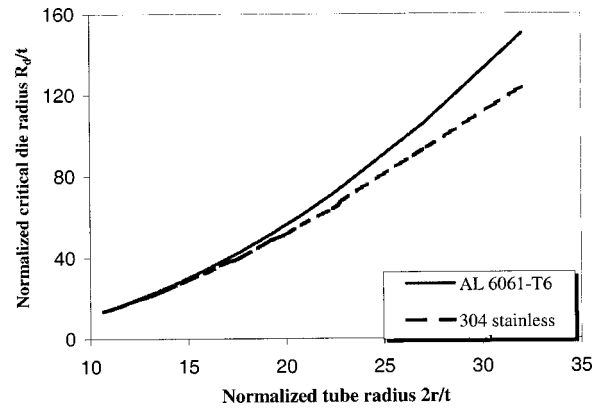


Fig. 6 Normalized critical die radius versus normalized tube radius for AL6061-T6 and 304 stainless steel

and  $\varepsilon_0=0$  while the material used in Fig. 5 is 304 stainless steel with  $K=1356$  MPa,  $n=0.549$ , and  $\varepsilon_0=0.001$ . It is illustrated in both materials that the minimum bending radius increases with an increase in tube radius and a decrease in tube thickness. In Li and Stelson [3], they did not observe the wrinkles in the bending of a tube with the tube thickness of 0.73 mm and tube radius  $r$  of 4.4 mm. The die radius they used is 28.7 mm. In our prediction, for such a case, the minimum bending radius without wrinkles should approximate 13.0 mm, which fits to their experimental observation.

Figure 6 displays the dependence of normalized critical die radius,  $R_d/t$ , on normalized tube radius,  $2r/t$  for AA6061-T6 and 304 stainless steel. For both materials, the normalized critical die radius tends to increase with tube radius. When the normalized tube radius  $2r/t$  is small, i.e., close to 10, there is no distinguishable difference between two materials. However, with increased  $2r/t$ , the steel shows lower critical die radius than AA6061-T6, i.e., has better formability in tube bending.

Figure 7 represents the effect of the strain hardening exponent  $n$  on the critical die radius. In Fig. 7, the parameters used are  $t=0.7$  mm,  $r=5$  mm and  $K=800$  MPa. It is seen that when the strain hardening exponent  $n$  is in the range between 0.05–0.25, which are typical values for most carbon steel and aluminum materials, critical die radius changes little with  $n$ . When  $n$  increases beyond 0.25, the critical die radius decreases dramatically. This also illustrates that the stainless steel with  $n=0.549$  has a lower critical die radius than aluminum as shown in Fig. 6.

Figure 8 investigates the effect of the strength coefficient  $K$  on the critical die radius. In Fig. 8, the parameters used are  $r=5$  mm,  $t=0.7$  mm, and  $n=0.2$ . The change of critical die radius with material strength coefficient  $K$  is relatively unnoticeable for material with a higher strength, i.e., when  $K$  is greater than around

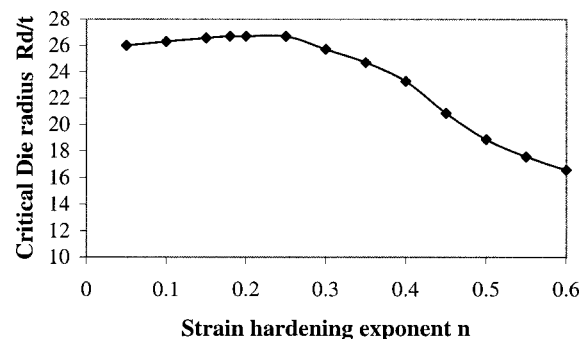


Fig. 7 Effect of strain hardening exponent  $n$  on critical die radius for  $t=0.7$  mm,  $r=5$  mm, and  $K=800$  MPa

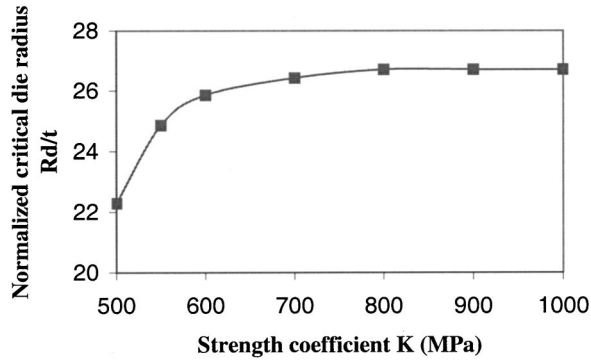


Fig. 8 Effect of strength coefficient  $K$  on critical die radius for  $r=5$  mm,  $t=0.7$  mm, and  $n=0.2$

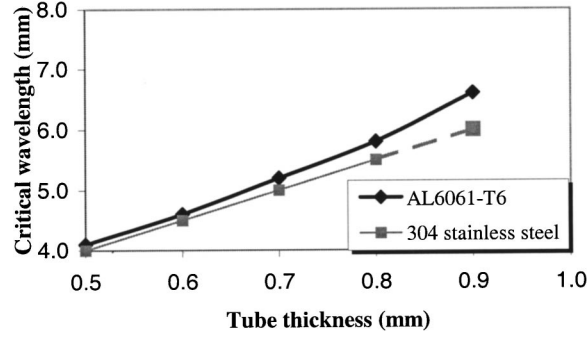


Fig. 9 Critical wavelength versus tube thickness under  $r=5$  mm for AL6061-T6 and 304 stainless steel

600 MPa. Only when  $K$  is lower than around 600 MPa, it can be seen that a higher  $K$  yields a higher critical die radius. It appears that the effect of strength coefficient  $K$  on critical die radius is relatively insignificant for most high strength materials.

It is found that the critical wavelength is almost independent of die radius for both AA6061-T6 and 304 stainless steel. However, the critical wavelength largely depends on tube thickness as shown in Fig. 9, where tube radius is 5 mm. The critical wavelength increases with thickness and AA6061-T6 has a little higher wavelength than stainless steel.

## Conclusions

The prediction of wrinkling in tube bending processes has been a challenging topic. The analysis of a curved tube can be characterized as buckling of a sheet with double curvatures. The analytical model for the onset of the wrinkling of an elastic-plastic doubly-curved sheet is developed in this paper using the energy method and the effective compressive area, which is the actual area under compression in the tube obtained from stress analysis either analytically or numerically. By defining the appropriate boundary conditions, the critical conditions can be obtained through energy equality.

A simple analytical model is established for the tube bending problem and the critical condition is obtained in terms of die radius and wavelength. It is found that the effects of tube radius and tube thickness are significant on the minimum die radius without the occurrence of wrinkling. The minimum bending radius increases with an increase in tube radius and a decrease in tube thickness. In addition, for most high strength material with a strain hardening exponent  $n$  lower than 0.25, the dependence of a minimum bending radius on material properties is relatively minor. This approach will provide a predictive tool in designing/optimizing the tooling and forming parameters and therefore may

eliminate the costly trial-and-error approach. Experiments on rotary-draw bending will be conducted to verify the present approach in the near future.

## Acknowledgments

The financial support for this work is from NSF grant No. DMI-9713744 and is greatly appreciated.

## Nomenclature

- $A, B, C$  = parameters in the Voce's law
- $E$  = elastic modulus
- $E_s, \nu_s$  = secant modulus and equivalent Poisson's ratio
- $E_{\alpha\beta}$  = stretching strains
- $I_{ni}, I_{\alpha}, I_{\theta}$  = parameters ( $i=0,2,4$ )
- $L_{\alpha\beta\kappa\gamma}$  = tangential moduli
- $\bar{L}_{\alpha\beta\kappa\gamma}$  = tangential moduli for plane stress condition
- $M_{\alpha\beta}$  = bending moments
- $N_{\alpha\beta}$  = membrane stress resultants
- $R$  = anisotropy parameter
- $R_d$  = bending die radius
- $b_{\alpha\beta}$  = curvature tensor of the middle surface
- $m, n$  = wave number in the hoop direction and lateral/radial direction
- $r$  = radius of tube
- $t$  = thickness of the plate
- $s_{ij}$  = stress deviator,  $i, j=1,2$
- $x, y, x_i$  = coordinates,  $i=1,2,3$
- $u_{\alpha}$  = displacements in the in-plane directions
- $w$  = normal deflection
- $w_0$  = deflection amplitude
- $\Delta T$  = external work done by membrane forces
- $\Delta U$  = bending energy
- $\sigma_{\alpha\beta}$  = stress components,  $\alpha, \beta=1,2$
- $\varepsilon_{\alpha\beta}$  = strain components
- $\delta_{ij}$  = Kronecker delta
- $\kappa_{\alpha\beta}$  = bending strains
- $\sigma_{y0}$  = initial yield stress
- $\sigma_x, \sigma_y$  = stress components
- $\bar{\sigma}$  = effective stress
- $\bar{\varepsilon}$  = effective strain
- $\Delta\alpha$  = bending angle
- $\alpha_i, \theta_i$  = span angle
- $\sigma_{\alpha}, \sigma_{\theta}$  = stress components in curvilinear coordinates
- $\nu$  = Poisson's ratio

## Appendix A

For a 3-D constitutive law with the form of  $\sigma_{\alpha\beta} = L_{\alpha\beta\kappa\gamma} \varepsilon_{\kappa\gamma}$ , the tangential moduli in the J2 deformation theory are given by

$$L_{ijkl} = \frac{E_s}{1 + \nu_s} \left[ \frac{1}{2} (\delta_{ik} \delta_{jl} + \delta_{il} \delta_{jk}) + \frac{\nu_s}{1 - 2\nu_s} \delta_{ij} \delta_{kl} - \frac{1}{q} s_{ij} s_{kl} \right] \quad (A1)$$

where  $s_{ij}$  is the stress deviator and  $\delta_{ij}$  denotes the Kronecker delta, the secant modulus  $E_s = \bar{\sigma} / \bar{\varepsilon}$ , and the equivalent Poisson's ratio  $\nu_s$  is obtained from

$$\frac{\nu_s}{E_s} = \frac{\nu}{E} + \frac{1}{2} \left( \frac{1}{E_s} - \frac{1}{E} \right) \quad (A2)$$

The parameter  $q$  is given as

$$q = \left[ (1 + \nu) \frac{2E_t}{3(E_s - E_t)} + 1 \right] \frac{2}{3} \bar{\sigma}^2 \quad (A3)$$

The incremental moduli for plane stress condition become

$$\bar{L}_{\alpha\beta\kappa\gamma} = L_{\alpha\beta\kappa\gamma} - \frac{L_{\alpha\beta 33} L_{33\kappa\gamma}}{L_{3333}} \quad (A4)$$

The covariant derivative of the deflection is

$$w_{,rr} = w_{,r\theta} = w_{,r\alpha} = 0 \quad (A5)$$

$$w_{,\theta\theta} = \frac{1}{r^2} \frac{\partial^2 w}{\partial \theta^2} \quad (A6)$$

$$w_{,\alpha\alpha} = \frac{1}{R^2} \frac{\partial^2 w}{\partial \alpha^2} - \frac{\cos \theta}{r^2} \frac{\partial w}{\partial \theta} \quad (A7)$$

$$w_{,\alpha\theta} = \frac{1}{rR'} \frac{\partial^2 w}{\partial \theta \partial \alpha} + \frac{\cos \theta}{R'^2} \frac{\partial w}{\partial \alpha} \quad (A8)$$

## References

- [1] Altan, T., et al., 1999, "Formability and Design Issues in Tube Hydroforming," *Hydroforming of Tube, Extrusions and Sheet Metal*, Vol. 1, K. Siegert, ed., pp. 105–121.
- [2] Stelson, K. A., and Lou, H., 1995, "Tolerance Analysis of Three-dimensional Tube Bending: Worst Case and Statistical Methods," *Transactions of NAMRI, SME, XXIII*, pp. 293–298.
- [3] Li, H. Z., Fageron, R., and Stelson, K. A., 1994, "A Method of Adaptive Control of Rotary-draw Thin-walled Tube Bending with Springback Compensation," *Transactions of NAMRI, SME, XXII*, pp. 25–28.
- [4] Shanley, F. R., 1947, "Inelastic column theory," *J. Aeronaut. Sci.*, **14**, pp. 261–267.
- [5] Hutchinson, J. W., and Neale, K. W., 1985, "Wrinkling of Curved Thin Sheet Metal," *Plastic Instability*, Presses Ponts et Chaussées, Paris, pp. 71–78.
- [6] Neale, K. W., and Tuğcu, P., 1990, "A Numerical Analysis of Wrinkle Formation Tendencies in Sheet Metals," *Int. J. Numer. Methods Eng.*, **30**, pp. 1595–1608.
- [7] Fatnassi, A., Tomita, Y., and Shindo, A., 1985, "Non-axisymmetric Buckling Behavior of Elastic-plastic Circular Tubes subjected to a Nosing Operation," *Int. J. Mech. Sci.*, **27**, pp. 643–651.
- [8] Corona, E., and Kyriakides, S., 1988, "On the collapse of inelastic tubes under combined bending and pressure," *Int. J. Solids Struct.*, **24**, pp. 505–535.
- [9] Ju, G. T., and Kyriakides, S., 1992, "Bifurcation and localization instabilities in cylindrical shells under bending -II: prediction," *Int. J. Solids Struct.*, **29**, No. 9, pp. 1143–1171.
- [10] Kyriakides, S., and Ju, G. T., 1992, "Bifurcation and localization instabilities in cylindrical shells under bending -I: experiments," *Int. J. Solids Struct.*, **29**, No. 9, pp. 1117–1142.
- [11] Corona, E., and Vaze, S. P., 1996, "Buckling of elastic-plastic square tubes under bending," *Int. J. Mech. Sci.*, **38**, No. 7, pp. 753–775.
- [12] Wang, X., and Cao, J., 1999, "On the onset of wrinkling of sheet with in-plane curvatures and without normal constraint," *Transaction of North American Manufacturing Research Conference, SME, XXVII*, pp. 55–60.
- [13] Wang, X., and Cao, J., 2000, "On the prediction of side-wall wrinkling in sheet metal forming processes," *Int. J. Mech. Sci.*, **42**, No. 12, pp. 2369–2394.
- [14] Wang, X., and Cao, J., 2001, "Wrinkling analysis in shrink flanging," to appear *J. Manuf. Sci. Eng.*, August.
- [15] Cao, J., and Wang, X., 1999, "An Analytical Model for Plate Wrinkling under Tri-axial Loading and Its Application," *Int. J. Mech. Sci.*, **42**, No. 3, pp. 617–633.
- [16] Wang, X., and Cao, J., 2000, "An analytical model for flange wrinkling in sheet metal forming," *Journal of Manufacturing Processes*, **2**, No. 2, pp. 100–107.
- [17] Timoshenko, S., 1961, *Theory of Elastic Stability*, McGraw-Hill, New York.